

Published in final edited form as:

Circ Res. 2012 August 17; 111(5): 521–531. doi:10.1161/CIRCRESAHA.112.265736.

Direct and indirect involvement of microRNA-499 in clinical and experimental cardiomyopathy

Scot J Matkovich, Yuanxin Hu, William H Eschenbacher, Lisa E Dorn, and Gerald W Dorn II
Center for Pharmacogenomics, Department of Internal Medicine, Washington University School of Medicine, St. Louis, MO 63110, USA

Abstract

Rationale—MicroRNA-499 and other members of the myomiR family regulate myosin isoforms in pressure overload hypertrophy. miR-499 expression varies in human disease but results of mouse cardiac miR-499 overexpression are inconsistent, either protecting against ischemic damage or aggravating cardiomyopathy after pressure overload. Likewise, there is disagreement over direct and indirect cardiac mRNAs targeted *in vivo* by miR-499.

Objectives—1. Define the associations between regulated miR-499 level in clinical and experimental heart disease and modulation of its predicted mRNA targets. 2. Determine the consequences of increased cardiac miR-499 on direct mRNA targeting, indirect mRNA modulation, and on myocardial protein content and post-translational modification.

Methods and Results—miR-499 levels were increased in failing and hypertrophied human hearts, and associated with decreased levels of predicted target mRNAs. Likewise, miR-499 is increased in Gq-mediated murine cardiomyopathy. Forced cardiomyocyte expression of miR-499 at levels comparable to human cardiomyopathy induced progressive murine heart failure and exacerbated cardiac remodeling after pressure overloading. Genome-wide RISC- and RNA-sequencing identified 67 direct, and numerous indirect, cardiac mRNA targets including Akt and MAPKs. Myocardial proteomics identified alterations in protein phosphorylation linked to the miR-499 cardiomyopathy phenotype, including of HSP90 and PP1 α .

Conclusions—miR-499 is increased in human and murine cardiac hypertrophy and cardiomyopathy, is sufficient to cause murine heart failure, and accelerates maladaptation to pressure overloading. The deleterious effects of miR-499 reflect the cumulative consequences of direct and indirect mRNA regulation, modulation of cardiac kinase and phosphatase pathways, and higher order effects on post-translational modification of myocardial proteins.

Keywords

microRNA; myomiR; gene silencing; pressure overload

MicroRNA (miR) 499 is one of three members of the myomiR family of microRNAs that coordinately regulate myosin isoform expression in cardiac hypertrophy. Gene knockout

Corresponding author: Gerald W Dorn II or Scot J Matkovich: Gerald W Dorn II, MD, Philip and Sima K Needleman Professor, Department of Internal Medicine and Center for Pharmacogenomics, 660 S. Euclid Ave., Campus Box 8220, St. Louis, MO 63110. Phone: 314-362-4892, FAX: 314-362-8844, gdorn@dom.wustl.edu. Scot J Matkovich, PhD, Assistant Professor, Department of Internal Medicine and Center for Pharmacogenomics, 660 S. Euclid Ave., Campus Box 8220, St. Louis, MO 63110. Phone: 314-747-3455, FAX: 314-362-8844, smatkovi@dom.wustl.edu.

The authors declare that they have no conflicts of interest relating to this manuscript.

Disclosures
none

studies have shown that miR-499 is functionally redundant with another myomiR, miR-208b, for regulating myosin gene expression¹. Transgenic overexpression studies have described either cardioprotection by miR-499 targeting of pro-hypertrophic calcineurin², or cardiac dysfunction by miR-499 regulation of early stress response genes³. Thus, the function of miR-499 in the heart, and the consequences of its regulated expression, are unclear.

miR-499 is highly expressed in hearts, but the mRNA of its parent *Myh7b* gene is not^{1, 3, 4}. miR-499 is encoded within intron 19 of *Myh7b*, a sarcomeric myosin gene expressed in skeletal muscle, but not significantly in hearts⁵. Cardiac miR-499 expression is uncoupled from *Myh7b* by alternative splicing of the primary transcript; *Myh7b* mRNA is eliminated by nonsense-mediated decay while miR-499 is protected by nuclear export⁵. The observation that hearts retain and dynamically regulate miR-499 at the expense of first transcribing, and then actively eliminating, the parent *Myh7b* mRNA suggests an important function in this organ.

Here, we describe miR-499 upregulation in diseased human and mouse hearts that is disproportionate to regulation of other myomiRs. We show that a number of bioinformatically-defined miR-499 target mRNAs are counter-regulated in the same samples. Using a combination of unbiased genome-wide “omics” approaches we define direct and indirect targets of miR-499, uncovering higher order effects not predicted by standard bioinformatics approaches and revealing systemic control by miR-499 over protein phosphorylation pathways.

Methods

miR and mRNA expression analysis in human and murine cardiomyopathy using microarrays has been previously described^{4, 6, 7}. Full details are in the Online Information.

Generation and characterization of miR-499 transgenic mice

miR-499 transgenic mice were created as described⁸; the studies here utilize the previously described mouse, designated line 1⁸ and referred to as TG-16 here, and two novel lines. Mice were housed according to procedures approved by the Washington University Institutional Animal Care and Use Committee. miR-499 expression was measured using NCode miR RT-qPCR system (Invitrogen) and detected using Sybr GreenER (Invitrogen). Histological examination, M-mode echocardiography of nonsedated mice, and surgical transverse aortic constriction, were carried out according to standard techniques⁹.

Identification and quantification of RISC-associated mRNAs and cardiac transcriptional profiling by high-throughput sequencing was performed as described^{7, 10}. Highly detailed experimental protocols are in the Online Information, including the ‘Appendix on RNA-sequencing’.

Proteomics and phosphoproteomics

2D DiGE (differential in-gel electrophoresis) total protein and phosphoproteome analyses, together with mass spectrometric protein identification, were performed as described¹¹ at Applied Biomics (Hayward, CA), using 5 pairs of nontransgenic and miR-499 TG-16 mouse hearts. Studies were performed at 8 weeks of age (at a time when miR-499 cardiomyopathy was evident by echocardiographic examination, but before overt heart failure had developed), and at 1 week after surgical transverse aortic coarctation. Detailed experimental protocols are in the Online Information.

Statistical and informatics analysis

Unless otherwise specified, all data are presented as mean \pm s.e.m and P-values were calculated using Student's unpaired t-test (for two groups) or 1-way ANOVA (for more than 2 groups). Statistical significance was taken at $P < 0.05$. Comparison of transcriptomic data sets, including calculation of false discovery rates, was performed using Partek Genomics Suite 6.5; significance was taken at $P < 0.005$ ($FDR < 0.05$). Gene-ontology analysis was performed using BiNGO¹². The online software suite MetaCore¹³ was also used to perform gene characterization and enrichment analyses; data herein derive from proprietary 'Pathway Maps', 'Process Networks' and 'Enrichment by Protein Function' modules. Full procedures for conversion of raw sequence reads to mRNA expression data are detailed in the Online Information in the 'Appendix on RNA-sequencing'.

Results

MyomiRs are increased in human and experimental cardiomyopathy and downregulate cardiac mRNA targets

MyomiRs are reportedly upregulated in human heart failure as part of a broader genetic program involving dozens of miRs and mRNAs^{4, 14}. Many such studies use 'failing' samples from explanted hearts at the time of transplantation, compared to 'non-failing' hearts harvested, but not used, for transplantation. Importantly, non-failing is not necessarily 'normal', and we have noted that hypertrophied non-failing human hearts have an abnormal gene expression signature⁴. Here we compared myomiR levels in normal, failing, and two available non-failing hypertrophied hearts. Compared to miR-208 (a and b) (Figure 1a, left panel), miR-499 was more aggressively upregulated in heart failure and hypertrophy (Figure 1a, right panel, blue circles and red triangles, respectively). Measurable miR-499 parent *Myh7b* transcript was also increased (Figure 1b, blue circles). Although the number of hypertrophied/non-failing samples is insufficient for statistical comparisons, these data suggest that miR-499 is upregulated in clinical hypertrophy and heart failure.

We examined the human heart transcriptomes for evidence of biological effects of increased miR-499. Recognizing that counter-regulation of target mRNAs is potentially influenced by other factors, we nevertheless considered that absence of such counter-regulation would show that miR-499 levels had little impact on the human condition. Steady-state levels of 98 cardiac-expressed miR-499 mRNA targets predicted by TargetScan6¹⁵ were significantly ($P < 0.05$) depressed in the same cardiomyopathic human hearts (Figure 1c; Online Table I). Thus, miR-499 and its parent *Myh7b* transcript are increased in human cardiomyopathy, and miR-499 upregulation is associated with downregulation of putative cardiac mRNA targets.

The cardiac Gαq-overexpressing mouse is a genetic model of cardiomyopathy that recapitulates seminal aspects of pressure overload hypertrophy^{16, 17}. To determine if increased miR-499 was a cell-autonomous response to a cardiomyocyte-specific cardiomyopathic stimulus we performed miR microarray analyses on hearts of four Gαq transgenic mice and four littermate controls⁶. miR-499 was increased 2.7-fold over control levels in Gαq hearts, and was the second most highly regulated microRNA in this model (Figure 1d). Cardiac miR-499 upregulation was validated in a separate Gαq cohort using miR RT-qPCR (Figure 1e). Thirteen cardiac miR-499 mRNA targets⁷ were correspondingly downregulated (Figure 1f), including the counter-regulated human heart failure miR-499 target, *Sos2* (Figure 1f, **asterisk**).

Forced cardiac miR-499 expression induces heart failure in mice

Previous mouse transgene expression studies have described both miR-499 mediated cardioprotection from ischemic injury² and miR-499 mediated induction and exacerbation

of heart failure³. Based on these results and our own observation that miR-499 is increased in heart disease, the conclusion is either that miR-499 is protective or detrimental. To help resolve this debate we forced expression of miR-499 in three independent lines of transgenic mouse hearts: two lines with levels observed in human heart failure (transgenic mouse lines TG-15 and TG-16, designated by their fold-expression) and one line with ~three-fold greater levels (TG-53) (Figure 2a; Online Figure I). miR-499 induced progressive cardiac enlargement and contractile dysfunction in all three lines; overt dilated cardiomyopathy was observed after 20 weeks of age (Figures 2b and 2c, Online Table II). Ventricular cardiomyocyte cross-sectional area increased in all three miR-499 transgenic lines (Figure 2d). Fibrosis was not a major component of the unstressed miR-499 phenotype, although limited areas of interstitial collagen were observed in aging mice of miR-499 TG-53 (Online Figure II).

miR-499 induced genetic re-programming typical of murine cardiac hypertrophy/heart failure¹⁸ (Figure 3a). Of hundreds of mRNAs altered in either 4 week or 8 week old miR-499 hearts, we identified 136 mRNAs that are concordantly regulated at both time points (thus filtering out the transcriptional background of normal postnatal heart growth)¹⁹. These results were consistent across individual mice, by genotype, and over time (Figure 3b, Online Table III). We designated this subset of regulated mRNAs as those primarily affected (either directly or indirectly) by miR-499. Gene-ontology analysis revealed major effects on Development and Formation of Cytoskeletal Elements (annotated as Biopolymers) (Online Figure III). Among the down-regulated primarily affected mRNAs were 31 identified by TargetScan6 as potential direct miR-499 targets, 4 of which had been down-regulated in Gα_q transgenic hearts (Figure 3c; Online Table IV) and 7 of which had been downregulated in human cardiomyopathy (Figure 3c, **asterisks**). We^{7, 20} and others^{21, 22} have demonstrated the superiority of RNA-sequencing over microarray and RT-qPCR methods for precision, dynamic range and high-throughput characterization. Nonetheless, we validated three of these mRNAs using TaqMan RT-qPCR (Figure 3d). Thus, at levels observed in human disease, miR-499 induces heart failure in mice and counter-regulates many of the same predicted mRNA targets.

We also examined how increased miR-499 levels influence disease progression after transverse aortic constriction (TAC). TAC produced left ventricular remodeling in both miR-499 and nontransgenic mice (Figures 4a and 4b), but only miR-499 mice developed left ventricular dysfunction (Figure 4b). Corresponding deleterious effects of miR-499 on the response to TAC were observed at the organ and cellular levels: heart weight to body weight ratios were higher (Figure 4c), cardiomyocyte cross-sectional area was greater (Figure 4d), and myocardial fibrosis was more extensive (Figure 4e).

Transcriptional profiling of nontransgenic and miR-499 transgenic mice one week after TAC surgery interrogated molecular mechanisms of adverse cardiac remodeling. Because TAC surgery was performed on 8-week old mice and the miR-499 induced cardiomyopathy was developing at this age, the transcriptional signature of TAC miR-499 mice should reflect three separate events: 1. direct effects of miR-499 overexpression (see above); 2. secondary effects of the developing cardiomyopathy, and 3. the response to pressure overload superimposed on #1 and #2. Unexpectedly, the most revealing comparison of transcript signatures was between TAC nontransgenic mice (626 regulated mRNAs) and sham-operated miR-499 mice (1,168 regulated mRNAs): 290 mRNAs were similarly regulated. Principal components analysis showed the expected genetic re-programming in pressure-overloaded nontransgenic mice, but the mRNA profile of miR-499 transgenic mice overlapped substantially with that of TAC, regardless of genotype (Figure 4f). The only statistically significant additional effect of pressure overloading on miR-499 hearts was hyper-upregulation of *Pi3kr1*. Unsupervised hierarchical clustering of regulated mRNAs

distinguished sham from pressure-overloaded nontransgenic groups, but was unable to resolve miR-499 transgenic sham and pressure-overloaded groups (Online Figure IV). These findings reveal similar cardiac gene reprogramming by miR-499 and pressure overload, and confirm and extend previously reported detrimental effects of miR-499 on TAC mouse hearts³.

Functional analysis of direct and indirect miR-499 mRNA targets

MicroRNAs exert their end-organ effects via suppression of direct mRNA targets, and by secondary and tertiary effects that accrue through so-called ‘indirect’ targets. It is therefore not surprising that many miR-499 regulated mRNAs were not bioinformatically identified as direct mRNA targets¹⁵. To better understand the relationship between miR-499 function and phenotype, we used agnostic whole-genome RISC-Sequencing to identify relevant mRNA targets of miR-499 in normal mouse hearts^{10, 23}. RISC-associated mRNAs were quantified in 4 week-old mice of miR-499 TG-16 (an age when heart size and function are normal, thus avoiding potential confounding effects of age-related cardiomyopathy) (see Figure 2b). Sixty-three mRNAs were enriched by 25% or greater in miR-499 programmed cardiac RISCs (Figure 5a, Online Table V), including the validated miR-499 target, *Sox6*^{1, 5}. By extending our filtering criteria to include any mRNAs increased by >3-fold in RISCs alone we identified another 4 miR-499 targets, including *Med13 (Thrap1)*⁵ that functions in α MHC/ β MHC isoform switching²⁴. TG-53, expressing three-fold greater miR-499, exhibited only twice (or less) RISC enrichment of these mRNA targets, compared to TG-16, revealing a nonlinear relationship between miR-499 level, RISC targeting (i.e. RISC saturation).

miR-mediated destabilization of targeted mRNA can depress steady-state mRNA levels^{25, 26}. Indeed, levels of ~one-fourth of the miR-499 RISC-enriched mRNAs were significantly depressed in the corresponding miR-499 transgenic hearts (Figure 5b; Online Table VI). A small number (8) of miR-499 RISC-targeted mRNAs showed increased steady-state levels, reflecting either indirect effects or atypical miR-target interactions²⁷ (Figure 5b). The physical location of miR-499 binding sites within these biologically-defined mRNA targets was identified through sequence complementarity; most were localized within 3' UTRs (Figure 5c).

Gene-ontology analysis uncovered functional overlap between the 67 direct miR-499 target mRNAs identified by RISC-Seq and the 136 indirectly regulated, primarily affected mRNAs detected by RNA-Seq (see Figure 3b). The GO categories of Development and Formation of Cytoskeletal Elements plus the additional category of Regulation of RNA Polymerase II-Dependent Transcription) were significantly enriched (using BiNGO¹²) (Online Figure III). A more detailed molecular function analysis of protein functional categories (e.g. kinases, phosphatases, enzymes, transcription factors, proteases, ligands, and receptors) (using MetaCore¹³), identified one hyper-enriched (P=0.0004) functional class of direct miR-499 mRNAs: Kinases. Eight of the 67 direct miR-499 target mRNAs are kinases: *Bmp2k*, *Cpne3*, *Hipk1*, *Hipk2*, *Map3k2 (Mekk2)*, *Stk35*, *Taok1* and *Uhmk1*. Both *Hipk1* and *Hipk2* are nuclear-localized protein serine/threonine kinases whose regulation can affect transcription²⁸.

As only a small proportion of miR-499 regulated mRNAs are direct targets recruited to the RISC, we assessed the ontological function of the 1,168 mRNAs secondarily regulated in the developing cardiomyopathy induced by miR-499 (Online Figure IV). MetaCore ‘Pathway Maps’ and ‘Process Networks’ analysis identified increased representation of mRNAs in Cytoskeletal Remodeling, TGF and Wnt pathways in miR-499 hearts (and also in TAC hearts; Online Table VII). MEF2-related signaling, which is a central transcriptional regulator of cardiac hypertrophy²⁹, was also markedly regulated by miR-499. Strikingly,

the only significantly enriched MetaCore ‘Molecular Function’ category was Kinases (Online Table VIII): 33 kinase mRNAs were upregulated and 6 were downregulated (Online Table IX). Those miR-499 regulated mRNAs that were similarly regulated in pressure overload (Online Figure IV) were also enriched in kinases (Online Table IX). (mRNAs distinctly regulated by pressure overload were not enriched in any molecular function category, but were significantly disenriched for the category of receptors [Online Table IX]). Of note, the pro-survival kinase Akt was centrally impacted by miR-499. Akt itself is downregulated by miR-499, whereas the phosphatase Pten (which dephosphorylates the upstream Akt activator PtdIns(3,4,5)P₃) and the phosphatase Phlpp1 (which dephosphorylates and inactivates Akt at Ser473)³⁰ were increased (Online Table IX). Another key cardiac kinase, CaMKII δ ³¹, is downregulated in miR-499 transgenic hearts. By contrast, several elements of mitogen-activated protein kinase cascades (*Map2k3*, *Map3k5*, *Map3k6*, *Map4k2*, *Map4k4*, *Mapk14*, and *Mknk2*) are upregulated (Online Table IX). Thus, miR-499 exerts major direct and indirect effects on cardiac protein kinase and phosphatase expression.

Higher order miR-499 effects on the cardiac proteome and phosphoproteome

We determined the (primary and secondary) proteomic consequences of transcriptional reprogramming by miR-499 using two-dimensional differential in-gel electrophoresis (DiGE)^{11, 32}. Proteomics analyses were performed on 8 week old mouse hearts to compare with the pressure overload studies (see above). DiGE is an agnostic measure of cardiac protein content, but detects the most highly expressed myocardial proteins.³³ Of ~1000 distinct protein spots (representing different proteins, protein isoforms, or post-translationally modified forms) quantified in five independent paired analyses, 27±2% were regulated 20% or greater by miR-499 transgene (12% upregulated; 15% downregulated) (Online Figure V). Forty-six regulated protein spots matched between all five paired analyses were identified by mass spectroscopy (n=31) or manual comparison to published proteomic maps (n=15) (Figure 6, Online Table X, Online Figure V). Of these, the protein products of *Ckmt2*, *Mdh1*, *Mybpc3* (MyBP-C), *Pdha1* and *P4hb* consisted of multiple spots corresponding to post-translationally modified species^{34–36}, including differential phosphorylation for MyBP-C¹¹ and *Pdha1*³⁷ (Figure 6, Online Figure V).

mRNA and protein expression data were available for 30 individual unambiguously defined gene products (excluding the five which migrated as multiple species). Six of these were concordantly regulated at the mRNA and protein level, while eight exhibited no change in mRNA or protein in miR-499 transgenic hearts, compared to nontransgenic hearts (Figure 6). Eleven additional gene products were unchanged at the mRNA level, but downregulated by miR-499 in the protein studies (Figure 6), and five gene products exhibited opposing regulation of steady-state mRNA and protein (Figure 6). We performed parallel proteomic profiling 1 week after TAC surgery. There were few differences between miR-499 transgenic and nontransgenic experiments in the proteins we identified (Online Table XI).

Given the observed miR-499 regulation of kinase and phosphatase pathways mRNAs, we compared in a 2×2 design the cardiac phosphoproteomes of nontransgenic and miR-499 mice at baseline and 1 week after pressure overloading by TAC (Figure 7 and Online Figure VI). Five strikingly regulated phosphoproteins, and one which did not change between treatments (Ehd2), were detected and identified using mass spectrometry (Online Table XII). Phosphorylation of the chaperone protein HSP90 β (*Hsp90ab1*) was modified in sham-operated miR-499 transgenic hearts (Figure 7c, Online Table XII); corresponding HSP90 β total protein and mRNA levels were unchanged (Online Table XII). Phosphorylation of protein phosphatase 1 α (*Ppp1ca*) was markedly increased in pressure-overloaded miR-499 transgenic mouse hearts; PP1 α phosphorylation was nearly undetectable in the other groups and its mRNA levels did not change. As we identified HSP90 β and PP1 α phosphoproteins

using mass spectrometry, the differential phosphorylation of Hsp90 β and PP1 α was confirmed using 2D PAGE followed by immunoblotting (Figure 7b) and the immunoblot gels compared to phosphoprotein gels (Figures 7c, 7d). *Ndufa10* (a complex I subunit) phosphorylation resembled that of PP1 α . *Pgm2* (phosphoglucomutase-2) phosphorylation was decreased in nontransgenic TAC hearts, without change in mRNA; *Gpd1* (glycerol-3-phosphate dehydrogenase 1) phosphorylation was increased in nontransgenic TAC hearts and sham-operated miR-499 transgenic hearts (Online Table XII).

Discussion

Here, in studies of human heart failure and transgenic mice, we provide evidence that upregulation of miR-499 contributes to pathological aspects of heart failure through direct regulation of approximately 70 individual primary mRNA targets, and indirect regulation of a large number of cardiac mRNAs and proteins. miR-499 levels are increased in human heart failure and the mouse G α q transgenic model of cardiomyopathy, its forced expression at similar levels to human heart failure in normal mouse hearts induces cardiomyopathy, and increased miR-499 levels adversely affect the response to pressure overload of mouse hearts. These results support a pathological role for miR-499 in the heart, consistent with previous associative studies^{4,5} and observations in two lines of miR-499 transgenic mice created by the Srivastava laboratory³.

Our studies demonstrate that the genetic reprogramming induced by miR-499 upregulation recapitulates many aspects of pathological cardiac hypertrophy at the transcriptional, cellular and organ level. Whole-transcriptome analysis by RNA-sequencing showed a marked overlap between the profiles of pressure-overloaded hearts and those expressing miR-499, while the increase in myocyte size and decline in contractile performance characteristic of the hypertrophying heart could be induced by miR-499 overexpression alone. Since miR-499 levels were also increased in hypertrophied, non-failing human and murine G α q transgenic hearts, it appears that some pathological aspects of reactive hypertrophy are conferred, at least in part, by miR-499. Our observations elucidate novel mechanisms by which miR-499 can contribute to cardiac disease, but do not suggest that inhibiting miR-499 would have therapeutic efficacy. Previous studies have determined that miR-499 is functionally redundant with another myomiR, miR-208b.¹ For this reason, increased expression of either of these miRs can contribute to cardiac pathology, but both would need to be inhibited to prevent that pathology. Indeed, expression of both miR-208b and miR-499 is indirectly controlled by miR-208a, and anti-miR therapy directed against miR-208a was recently shown to improve experimental hypertrophy³⁸.

We integrated results of unbiased transcriptome and proteomic analyses to uncover a striking feature of miR-499 induced heart disease; regulation of pathways that orchestrate post-translational protein modification. Wang *et al.* implicated miR-499 translational suppression of the cardiac hypertrophy effector phosphatase, calcineurin in post-translational modification of the mitochondrial fission protein, dynamin-related protein 1 (Drp1)². Our unbiased comprehensive examination of direct and indirect miR-499 targets likewise suggests that many effects of this miR are mediated via regulation of kinase/phosphatase pathways (Figure 8). Kinases regulated directly and indirectly by miR-499, together with the observed altered phosphorylation of the key signaling proteins HSP90 β and PP1 α , influence mitogen-activated protein kinase (MAPK) cascades, control of mRNA translation, Ca²⁺ transport, and cell survival (Figure 8).

HSP90 β phosphorylation was directly affected by miR-499 (i.e. was altered in the absence of TAC). Constitutively expressed HSP90 β is expressed at higher levels than stress-inducible HSP90 α (gene symbol *Hsp90aa1*) in both heart and skeletal muscle^{39,40}.

Interestingly, *Hsp90aa1* mRNA was upregulated 1.5-fold by pressure overload alone (Online Table XII). Interactions of the HSP90 proteins with their co-chaperones and signaling proteins (such as Cdc37⁴¹ and PP5⁴²) is regulated by phosphorylation⁴³. Cardiac signaling most affected by HSP90 includes the p38 MAP kinase pathway⁴¹ and the cardiac ERG potassium channel⁴⁴. Importantly, HSP90 controls signaling through the “physiological hypertrophy” PI3K / Akt signaling axis by stabilizing both Akt⁴⁵ and its activating upstream kinase *Pdk1*⁴⁶. HSP90 may also directly affect miR functioning by facilitating maturation and targeting of Ago2 to P-bodies and miR-loaded RISC complexes⁴⁷; the extent to which these processes are affected by HSP90 phosphorylation has not been determined.

In contrast to modulation of HSP90 β phosphorylation by miR-499, PP1 α phosphorylation was only strongly detected with the combination of TAC and miR-499 overexpression. The ability of PP1 α to dephosphorylate substrates and regulate signal transduction depends on the presence of appropriate adapter proteins that target PP1 α to macromolecular complexes⁴⁸, but its phosphorylation interferes with its catalytic activity⁴⁹. Cardiac phosphoproteins regulated by PP1 α include RyRs⁵⁰, phospholamban⁵¹, IP₃Rs⁵² and the sodium/calcium exchanger Ncx1⁵³.

While the current results have provided fresh insight into the effects of miR-499 on the heart, and uncovered new mechanisms for those effects, a more general aim of our laboratory is to deploy more effective techniques for analyzing and understanding the consequences of regulated miRs in heart disease. As many miRs are encoded within introns of parent genes, and others have their own transcriptional regulatory mechanisms, it is not surprising that regulated expression of miRs occurs under many of the same circumstances as regulated expression of protein-coding mRNAs. We previously described concurrent regulation of miR and mRNAs in human heart failure, and observed that miRs appear more sensitive to the functional dynamics of heart failure clinical status⁴. Similar observations⁵⁴ and the more recent finding that miR are released into the blood stream and may serve as both signatures and systemic mediators of cardiac disease⁵⁵, have further catalyzed interest in defining the roles of individual miRs in the heart and other tissues. However, the convoluted targeting patterns of miRs, in which the effects of a single miR on multiple targets are multiplied through secondary and tertiary indirect effects, complicate their *in vivo* analysis. As an example, myomiRs are best known by their critical actions regulating cardiac myosin isoform expression in response to stress or hormonal factors^{1,24} yet our studies did not identify mRNAs for either *Myh6* or *Myh7* as RISC-enriched after miR-499 programming. In other words these two major targets of myomiRs are not directly recruited by miR-499 for destruction in the cardiac RISC, but represent indirect targets affected through secondary or tertiary mechanisms. This is consistent with Bartel's⁵⁶ observation that: ‘The (miR) responsive proteins are not necessarily the endogenous (miR) targets, and the magnitude and kinetics of mRNA and protein changes are not expected to match those of endogenous targeting.’ The majesty of microRNAs, and the potential utility of targeting them in disease, is their ability to regulate entire biological pathways in this way. We suggest that the reductionist paradigm of one molecule affecting one target that causes a given phenotype does not typically apply to miRs.

Despite similar cardiac phenotypes in response to miR-499 overexpression, our mRNA analyses reveal several differences to the studies of Shieh *et al.*³. Indeed, we⁷ and others²¹ have described greater specificity and accuracy of RNA sequencing over RNA microarrays, and it is likely that some of the discrepancies between the description of cardiac miR-499 mRNA targets by Shieh *et al.*³ and the current study derive from our different approaches to mRNA analysis (see Online Tables XIII and XIV) and potentially the difference in age of the mice used (postnatal day 17 compared to 4 week-old animals). Evidence of our technical

advantage in RNA analysis includes our observation that the well-described *in vitro* miR-499 target, *Sox6*, is indeed both recruited to the RISCs and downregulated in miR-499 overexpressing hearts, whereas Shieh *et al.*'s microarray analysis, and qPCR and immunoblot analyses relating *Sox6* to *Gapdh*, did not detect downregulation of *Sox6* in their miR-499 hearts³. We previously observed that *Sox6* is highly enriched in the RISCs of nontransgenic hearts (as expected from high endogenous miR-499 expression levels)¹⁰ and is further recruited to the RISCs of miR-499 transgenic hearts, although as previously discussed¹⁰, our more stringent selection criteria in the earlier study excluded *Sox6* from a miR-499-programmed, RISC-enriched gene list.

Although an agnostic, biologically driven approach has many advantages, we would like to emphasize certain limitations of RNA-sequencing and Argonaute 2 immunoprecipitation as employed herein. First, RISC programming by transgenic miR overexpression has the potential to express both the mature miR and its complement (miR*). If the overexpressed miR* is not eliminated in a normal manner, then it will recruit its targets to the RISC, which will be detected by RISC-sequencing. In our studies, we use RT-qPCR to measure the miR and miR* products of each tissue assayed; in the case of miR-499, we find that miR-499* (miR-499-3p) is expressed at levels ~600-fold below that of miR-499(-5p) and that this ratio remains similar in miR-499 transgenic mice (Yuanxin Hu and Gerald Dorn, unpublished data). Second, we think that overexpressing miRs that are already expressed at high levels may not be as effective in revealing their targets as RISC-programming with miRs expressed at more modest levels, because at some level miR-mRNA incorporation into the RISC will approach saturation. Indeed, saturability of the RISC with highly expressed miRs may explain the non-linear relationship between miR-499 expression level and phenotypic effect in our low and high expressing transgenic mice (Figures 2 and 5). Finally, it is conceivable that the expression level of other miRs will be altered by miR overexpression (or ablation), which will alter the RISCome accordingly. This scenario would incorrectly identify some RISC-enriched mRNAs as direct targets of the RISC-programming miR.

In summary, we have shown that miR-499 is highly upregulated in human heart disease, that forced cardiomyocyte miR-499 expression is sufficient to induce progressive heart failure in mice and that elevated miR-499 expression is deleterious in the context of pressure overload. The end-organ effects of miR-499 are complex, reinforcing the need to agnostically investigate miR-mRNA interactions and miR-regulated changes of protein content in the appropriate *in vivo* context.

Supplementary Material

Refer to Web version on PubMed Central for supplementary material.

Acknowledgments

Illumina raw sequencing data was generated at the Genome Technology Access Center in the Department of Genetics at Washington University School of Medicine. The Center is partially supported by NCI Cancer Center Support Grant #P30 CA91842 to the Siteman Cancer Center and by ICTS/CTSA Grant# UL1RR024992 from the National Center for Research Resources (NCRR), a component of the National Institutes of Health (NIH), and NIH Roadmap for Medical Research.

Sources of Funding

Supported by NIH/NHLBI R01 HL108943 and by a Fondation Leducq Transatlantic Network of Excellence in Cardiovascular Research Program.

Non-standard abbreviations and acronyms

miR	microRNA
RISC	RNA-induced silencing complex
DiGE	differential in-gel electrophoresis
FDR	false discovery rate
HSP90	heat shock protein 90 kDa (cytosolic)
PP1α	protein serine/threonine phosphatase 1 alpha
CnA	calcineurin A
Drp1	dynamamin-related protein 1

References

- van Rooij E, Quiat D, Johnson BA, Sutherland LB, Qi X, Richardson JA, Kelm RJ Jr, Olson EN. A family of microRNAs encoded by myosin genes governs myosin expression and muscle performance. *Dev Cell*. 2009; 17:662–673. [PubMed: 19922871]
- Wang JX, Jiao JQ, Li Q, Long B, Wang K, Liu JP, Li YR, Li PF. miR-499 regulates mitochondrial dynamics by targeting calcineurin and dynamamin-related protein-1. *Nat Med*. 2011; 17:71–78. [PubMed: 21186368]
- Shieh JT, Huang Y, Gilmore J, Srivastava D. Elevated miR-499 levels blunt the cardiac stress response. *PLoS One*. 2011; 6:e19481. [PubMed: 21573063]
- Matkovich SJ, Van Booven DJ, Youker KA, Torre-Amione G, Diwan A, Eschenbacher WH, Dorn LE, Watson MA, Margulies KB, Dorn GW 2nd. Reciprocal regulation of myocardial microRNAs and messenger RNA in human cardiomyopathy and reversal of the microRNA signature by biomechanical support. *Circulation*. 2009; 119:1263–1271. [PubMed: 19237659]
- Bell ML, Buvoli M, Leinwand LA. Uncoupling of expression of an intronic microRNA and its myosin host gene by exon skipping. *Mol Cell Biol*. 2010; 30:1937–1945. [PubMed: 20154144]
- Matkovich SJ, Wang W, Tu Y, Eschenbacher WH, Dorn LE, Condorelli G, Diwan A, Nerbonne JM, Dorn GW 2nd. MicroRNA-133a protects against myocardial fibrosis and modulates electrical repolarization without affecting hypertrophy in pressure-overloaded adult hearts. *Circ Res*. 2010; 106:166–175. [PubMed: 19893015]
- Matkovich SJ, Zhang Y, Van Booven D, Dorn GW 2nd. Deep mRNA sequencing for in vivo functional analysis of cardiac transcriptional regulators. Application to Gaq. *Circ Res*. 2010; 106:1459–1467. [PubMed: 20360248]
- Dorn GW 2nd, Matkovich SJ, Eschenbacher WH, Zhang Y. A human 3' miR-499 mutation alters cardiac mRNA targeting and function. *Circ Res*. 2012; 110:958–967. [PubMed: 22374132]
- Diwan A, Wansapura J, Syed FM, Matkovich SJ, Lorenz JN, Dorn GW 2nd. Nix-mediated apoptosis links myocardial fibrosis, cardiac remodeling, and hypertrophy decompensation. *Circulation*. 2008; 117:396–404. [PubMed: 18178777]
- Matkovich SJ, Van Booven DJ, Eschenbacher WH, Dorn GW 2nd. RISC RNA sequencing for context-specific identification of in vivo microRNA targets. *Circ Res*. 2011; 108:18–26. [PubMed: 21030712]
- Kang MY, Zhang Y, Matkovich SJ, Diwan A, Chishti AH, Dorn GW 2nd. Receptor-independent cardiac protein kinase Calpha activation by calpain-mediated truncation of regulatory domains. *Circ Res*. 2010; 107:903–912. [PubMed: 20689063]
- Maere S, Heymans K, Kuiper M. BiNGO: a Cytoscape plugin to assess overrepresentation of gene ontology categories in biological networks. *Bioinformatics*. 2005; 21:3448–3449. [PubMed: 15972284]
- GeneGo. [Accessed 4/2/12] MetaCore. Available at: <http://www.genego.com>
- Liu N, Olson EN. MicroRNA regulatory networks in cardiovascular development. *Dev Cell*. 2010; 18:510–525. [PubMed: 20412767]

15. Garcia DM, Baek D, Shin C, Bell GW, Grimson A, Bartel DP. Weak seed-pairing stability and high target-site abundance decrease the proficiency of lsy-6 and other microRNAs. *Nat Struct Mol Biol.* 2011; 18:1139–1146. [PubMed: 21909094]
16. D'Angelo DD, Sakata Y, Lorenz JN, Boivin GP, Walsh RA, Liggett SB, Dorn GW II. Transgenic Gaq overexpression induces cardiac contractile failure in mice. *Proc Natl Acad Sci USA.* 1997; 94:8121–8126. [PubMed: 9223325]
17. Adams JW, Sakata Y, Davis MG, Sah VP, Wang Y, Liggett SB, Chien KR, Brown JH, Dorn GW II. Enhanced Gaq signaling: A common pathway mediates cardiac hypertrophy and apoptotic heart failure. *Proc Natl Acad Sci USA.* 1998; 95:10140–10145. [PubMed: 9707614]
18. Dorn GW II, Robbins J, Sugden PH. Phenotyping hypertrophy - eschew obfuscation. *Circ Res.* 2003; 92:1171–1175. [PubMed: 12805233]
19. Syed F, Odley A, Hahn HS, Brunskill EW, Lynch RA, Marreez Y, Sanbe A, Robbins J, Dorn GW 2nd. Physiological growth synergizes with pathological genes in experimental cardiomyopathy. *Circ Res.* 2004; 95:1200–1206. [PubMed: 15539635]
20. Zhang Y, Matkovich SJ, Duan X, Diwan A, Kang MY, Dorn GW 2nd. Receptor-independent PKCa signaling by calpain-generated free catalytic domains induces HDAC5 nuclear export and regulates cardiac transcription. *J Biol Chem.* 2011; 286:24943–24951. [PubMed: 21543317]
21. Marioni JC, Mason CE, Mane SM, Stephens M, Gilad Y. RNA-seq: an assessment of technical reproducibility and comparison with gene expression arrays. *Genome Res.* 2008; 18:1509–1517. [PubMed: 18550803]
22. Mortazavi A, Williams BA, McCue K, Schaeffer L, Wold B. Mapping and quantifying mammalian transcriptomes by RNA-Seq. *Nat Methods.* 2008; 5:621–628. [PubMed: 18516045]
23. Porrello ER, Johnson BA, Aurora AB, Simpson E, Nam YJ, Matkovich SJ, Dorn GW 2nd, van Rooij E, Olson EN. miR-15 family regulates postnatal mitotic arrest of cardiomyocytes. *Circ Res.* 2011; 109:670–679. [PubMed: 21778430]
24. van Rooij E, Sutherland LB, Qi X, Richardson JA, Hill J, Olson EN. Control of stress-dependent cardiac growth and gene expression by a microRNA. *Science.* 2007; 316:575–579. [PubMed: 17379774]
25. Guo H, Ingolia NT, Weissman JS, Bartel DP. Mammalian microRNAs predominantly act to decrease target mRNA levels. *Nature.* 2010; 466:835–840. [PubMed: 20703300]
26. Standart N, Jackson RJ. MicroRNAs repress translation of m7Gppp-capped target mRNAs in vitro by inhibiting initiation and promoting deadenylation. *Genes Dev.* 2007; 21:1975–1982. [PubMed: 17699746]
27. Buchan JR, Parker R. Molecular biology. The two faces of miRNA. *Science.* 2007; 318:1877–1878. [PubMed: 18096794]
28. Rinaldo C, Siepi F, Prodosmo A, Soddu S. HIPKs: Jack of all trades in basic nuclear activities. *Biochim Biophys Acta.* 2008; 1783:2124–2129. [PubMed: 18606197]
29. Czubryt MP, Olson EN. Balancing contractility and energy production: the role of myocyte enhancer factor 2 (MEF2) in cardiac hypertrophy. *Recent Prog Horm Res.* 2004; 59:105–124. [PubMed: 14749499]
30. Miyamoto S, Purcell NH, Smith JM, Gao T, Whittaker R, Huang K, Castillo R, Glembotski CC, Sussman MA, Newton AC, Brown JH. PHLPP-1 negatively regulates Akt activity and survival in the heart. *Circ Res.* 2010; 107:476–484. [PubMed: 20576936]
31. Zhang T, Miyamoto S, Brown JH. Cardiomyocyte calcium and calcium/calmodulin-dependent protein kinase II: friends or foes? *Recent Prog Horm Res.* 2004; 59:141–168. [PubMed: 14749501]
32. Fleissner F, Jazbutyte V, Fiedler J, Gupta SK, Yin X, Xu Q, Galuppo P, Kneitz S, Mayr M, Ertl G, Bauersachs J, Thum T. Short communication: asymmetric dimethylarginine impairs angiogenic progenitor cell function in patients with coronary artery disease through a microRNA-21-dependent mechanism. *Circ Res.* 2010; 107:138–143. [PubMed: 20489163]
33. Raddatz K, Albrecht D, Hochgrafe F, Hecker M, Gotthardt M. A proteome map of murine heart and skeletal muscle. *Proteomics.* 2008; 8:1885–1897. [PubMed: 18398877]
34. Zhao S, Xu W, Jiang W, Yu W, Lin Y, Zhang T, Yao J, Zhou L, Zeng Y, Li H, Li Y, Shi J, An W, Hancock SM, He F, Qin L, Chin J, Yang P, Chen X, Lei Q, Xiong Y, Guan KL. Regulation of

- cellular metabolism by protein lysine acetylation. *Science*. 2010; 327:1000–1004. [PubMed: 20167786]
35. Grillon JM, Johnson KR, Kotlo K, Danziger RS. Non-histone lysine acetylated proteins in heart failure. *Biochim Biophys Acta*. 2011
 36. Banfi C, Brioschi M, Barcella S, Veglia F, Biglioli P, Tremoli E, Agostoni P. Oxidized proteins in plasma of patients with heart failure: role in endothelial damage. *Eur J Heart Fail*. 2008; 10:244–251. [PubMed: 18331966]
 37. Kato M, Chuang JL, Tso SC, Wynn RM, Chuang DT. Crystal structure of pyruvate dehydrogenase kinase 3 bound to lipoyl domain 2 of human pyruvate dehydrogenase complex. *EMBO J*. 2005; 24:1763–1774. [PubMed: 15861126]
 38. Montgomery RL, Hullinger TG, Semus HM, Dickinson BA, Seto AG, Lynch JM, Stack C, Latimer PA, Olson EN, van Rooij E. Therapeutic inhibition of miR-208a improves cardiac function and survival during heart failure. *Circulation*. 2011; 124:1537–1547. [PubMed: 21900086]
 39. Grad I, Cederroth CR, Walicki J, Grey C, Barluenga S, Winssinger N, De Massy B, Nef S, Picard D. The molecular chaperone Hsp90alpha is required for meiotic progression of spermatocytes beyond pachytene in the mouse. *PLoS One*. 2010; 5:e15770. [PubMed: 21209834]
 40. Sreedhar AS, Kalmar E, Csermely P, Shen YF. Hsp90 isoforms: functions, expression and clinical importance. *FEBS Lett*. 2004; 562:11–15. [PubMed: 15069952]
 41. Ota A, Zhang J, Ping P, Han J, Wang Y. Specific regulation of noncanonical p38alpha activation by Hsp90-Cdc37 chaperone complex in cardiomyocyte. *Circ Res*. 2010; 106:1404–1412. [PubMed: 20299663]
 42. Wandinger SK, Suhre MH, Wegele H, Buchner J. The phosphatase Ppt1 is a dedicated regulator of the molecular chaperone Hsp90. *EMBO J*. 2006; 25:367–376. [PubMed: 16407978]
 43. Mollapour M, Neckers L. Post-translational modifications of Hsp90 and their contributions to chaperone regulation. *Biochim Biophys Acta*. 2012; 1823:648–655. [PubMed: 21856339]
 44. Ficker E, Dennis AT, Wang L, Brown AM. Role of the cytosolic chaperones Hsp70 and Hsp90 in maturation of the cardiac potassium channel HERG. *Circ Res*. 2003; 92:e87–100. [PubMed: 12775586]
 45. Basso AD, Solit DB, Chiosis G, Giri B, Tschlis P, Rosen N. Akt forms an intracellular complex with heat shock protein 90 (Hsp90) and Cdc37 and is destabilized by inhibitors of Hsp90 function. *J Biol Chem*. 2002; 277:39858–39866. [PubMed: 12176997]
 46. Fujita N, Sato S, Ishida A, Tsuruo T. Involvement of Hsp90 in signaling and stability of 3-phosphoinositide-dependent kinase-1. *J Biol Chem*. 2002; 277:10346–10353. [PubMed: 11779851]
 47. Pare JM, Tahbaz N, Lopez-Orozco J, LaPointe P, Lasko P, Hobman TC. Hsp90 regulates the function of argonaute 2 and its recruitment to stress granules and P-bodies. *Mol Biol Cell*. 2009; 20:3273–3284. [PubMed: 19458189]
 48. Brautigam DL. Protein Ser/Thr phosphatases : the ugly ducklings of cell signaling. *FEBS J*. 2012 in press.
 49. Dohadwala M, da Cruz e Silva EF, Hall FL, Williams RT, Carbonaro-Hall DA, Nairn AC, Greengard P, Berndt N. Phosphorylation and inactivation of protein phosphatase 1 by cyclin-dependent kinases. *Proc Natl Acad Sci USA*. 1994; 91:6408–6412. [PubMed: 8022797]
 50. Marx SO, Reiken S, Hisamatsu Y, Gaburjakova M, Gaburjakova J, Yang Y-m, Rosemblyt N, Marks AR. Phosphorylation-dependent regulation of ryanodine receptors: a novel role for leucine/isoleucine zippers. *J Cell Biol*. 2001; 153:699–708. [PubMed: 11352932]
 51. Pathak A, del Monte F, Zhao W, Schultz JE, Lorenz JN, Bodi I, Weiser D, Hahn H, Carr AN, Syed F, Mavila N, Jha L, Qian J, Marreez Y, Chen G, McGraw DW, Heist EK, Guerrero JL, DePaoli-Roach AA, Hajjar RJ, Kranias EG. Enhancement of cardiac function and suppression of heart failure progression by inhibition of protein phosphatase 1. *Circ Res*. 2005; 96:756–766. [PubMed: 15746443]
 52. deSouza N, Reiken S, Ondrias K, Yang Y-m, Matkovich S, Marks AR. Protein kinase A and two phosphatases are components of the inositol 1,4,5-trisphosphate receptor macromolecular signaling complex. *J Biol Chem*. 2002; 277:39397–39400. [PubMed: 12167631]

53. Schulze DH, Muqhal M, Lederer WJ, Ruknudin AM. Sodium/calcium exchanger (NCX1) macromolecular complex. *J Biol Chem.* 2003; 278:28849–28855. [PubMed: 12754202]
54. Thum T, Galuppo P, Wolf C, Fiedler J, Kneitz S, van Laake LW, Doevendans PA, Mummery CL, Borlak J, Haverich A, Gross C, Engelhardt S, Ertl G, Bauersachs J. MicroRNAs in the human heart: a clue to fetal gene reprogramming in heart failure. *Circulation.* 2007; 116:258–267. [PubMed: 17606841]
55. Fichtlscherer S, Zeiher AM, Dimmeler S. Circulating microRNAs: biomarkers or mediators of cardiovascular diseases? *Arterioscler Thromb Vasc Biol.* 2011; 31:2383–2390. [PubMed: 22011751]
56. Baek D, Villen J, Shin C, Camargo FD, Gygi SP, Bartel DP. The impact of microRNAs on protein output. *Nature.* 2008; 455:64–71. [PubMed: 18668037]
57. Vandesompele J, De Preter K, Pattyn F, Poppe B, Van Roy N, De Paepe A, Speleman F. Accurate normalization of real-time quantitative RT-PCR data by geometric averaging of multiple internal control genes. *Genome Biol.* 2002; 3:RESEARCH0034.0031–0012. [PubMed: 12184808]

Novelty and Significance

What is Known?

- MicroRNAs (miRs) suppress their target mRNAs by recruiting them to RNA-induced silencing complexes, inhibiting translation and/or causing mRNA degradation
- miR-499 is regulated in human heart disease
- Studies to date have been divided on whether miR-499 is beneficial or detrimental to cardiac function and have also disagreed on which mRNAs are targeted by miR-499

What New Information does this Article Contribute?

- miR-499 is upregulated in failing and hypertrophied human hearts and in a genetic model of murine cardiomyopathy
- Cardiac overexpression of miR-499 in multiple lines of mice induced cardiomyopathy, and worsened the response to pressure overload
- Direct and indirect targets of miR-499 were defined using transcriptome-wide RISC and RNA sequencing, together with proteomic studies which revealed regulation of protein phosphorylation in miR-499 cardiomyopathy

We demonstrate here that miR-499 is upregulated in human heart failure and in the $G\alpha_q$ model of murine cardiomyopathy. Its overexpression in the murine heart at levels similar to those in human heart failure was sufficient to induce cardiomyopathy in multiple transgenic lines, and exacerbated the response to pressure overload. To determine the *in vivo* targets of miR-499, we performed rigorous, transcriptome-wide and quantitative RISC and RNA sequencing on miR-499 transgenic hearts. Although miR-499 is a member of the myomiR family that derive from and ultimately regulate cardiac myosins, no myosin isoforms were recruited to the RISC. Rather, through direct targeting of 67 mRNAs and indirect regulation of another ~1,000, miR-499 exerts complex effects on the cardiac transcriptome, particularly targeting kinases and phosphatases. Myocardial proteomics revealed alteration in the levels of a myriad of proteins, several of which were identified with mass spectrometry or reference to proteomic maps. Of particular note, considering the effect of miR-499 on members of phosphorylation cascades, were altered HSP90 β and PP1 α phosphorylation. Overall, we have shown that excess miR-499 is detrimental to the heart and that upregulation of even a single miR has far-reaching consequences on the myocardial transcriptome, proteome and its post-translational modification.

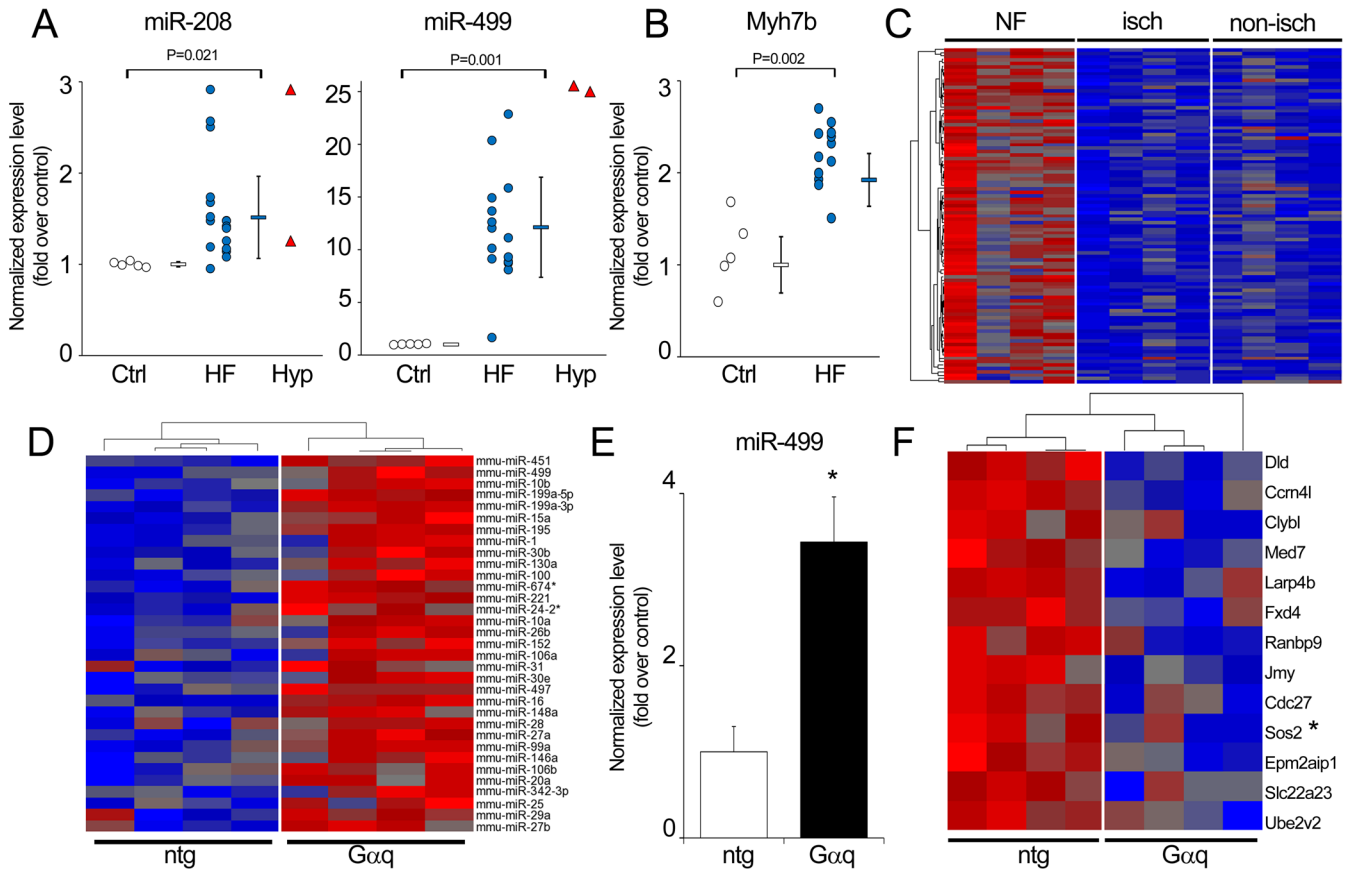


Figure 1. miR-499 upregulation and target suppression in human heart failure and murine genetic cardiomyopathy

(A) Increased miR-208, miR-499 levels in human heart failure; white = non-failing (Ctrl), blue = failing hearts (HF), red = hypertrophied non-failing hearts (Hyp). The miR expression arrays used did not distinguish between miRs-208a and -208b. Individual data are shown together with mean \pm s.d. (B) Increased *Myh7b* levels in human heart failure; white = non-failing (Ctrl) and blue = failing hearts (HF). (C) Downregulation of 98 miR-499 target mRNAs, predicted by TargetScan, in human heart failure (greater than 1.2-fold downregulation, $P < 0.05$, Online Table I). Four representative hearts each are shown for non-failing (NF), and failing hearts with cardiomyopathy of ischemic origin (isch) or non-ischemic origin (non-isch). Red = higher expression, blue = lower expression. (D) miR microarray analysis of *Gαq* transgenic hearts⁶, displaying miRs according to degree of upregulation (1.2-fold or greater, $P < 0.05$; miR-451, 4.4 fold-upregulated in *Gαq*, is at the top). (E) miR-499 analyzed by RT-qPCR relative to combined reference of 5S rRNA, U6 snRNA and *Gapdh* mRNA⁵⁷ in nontransgenic ($n=3$) and *Gαq* hearts ($n=6$). Data shown are mean \pm s.e.m., arbitrary units (nontransgenic = 1); * denotes $P=0.0006$, 2-tailed unpaired t-test. (F) Downregulation of 13 miR-499 target mRNAs, predicted by TargetScan (greater than 1.2-fold downregulation, $P < 0.05$) in *Gαq* transcriptomes analyzed by RNA-sequencing⁷. Red, higher expression; blue, lower expression. * denotes downregulation of the same mRNA in human heart failure.

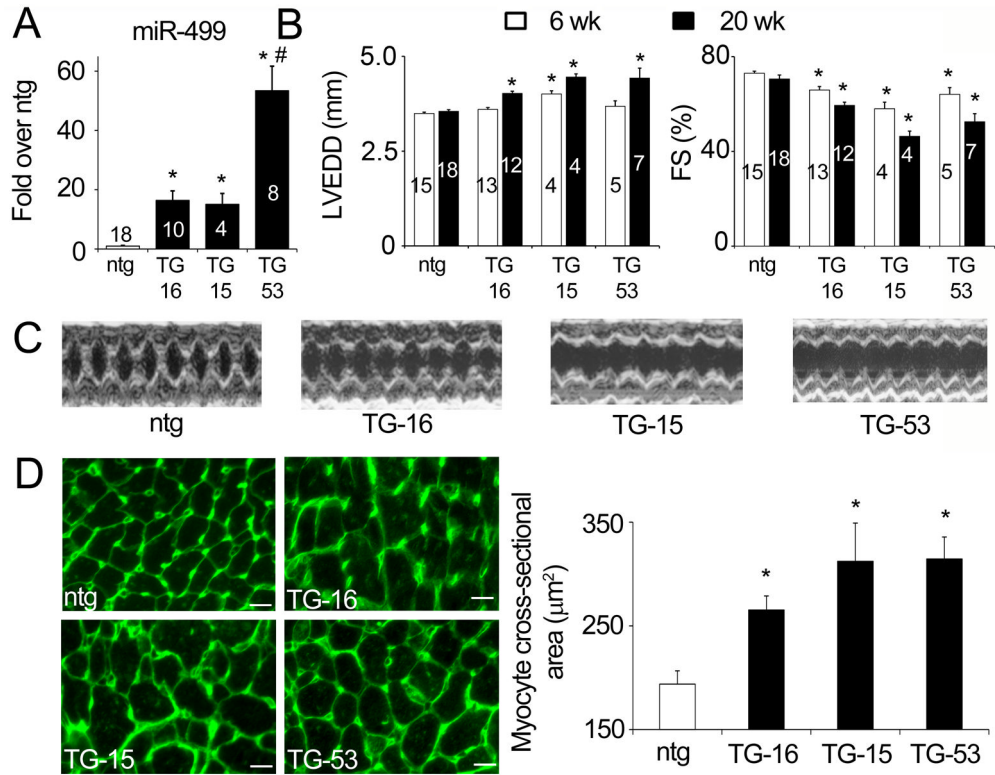


Figure 2. Cardiac miR-499 overexpression causes heart failure in mice

(A) Cardiac-directed overexpression of miR-499 in two transgenic mouse lines at levels similar to human heart failure (TG-16 and TG-15) and in a higher-overexpressing line (TG-53). * denotes $P < 0.0001$ relative to nontransgenic (1-way ANOVA); # denotes significant difference to all other groups (Tukey's pairwise comparisons). (B) Progressive dilated cardiomyopathy in miR-499 transgenic hearts shown by increases in left-ventricular end-diastolic dimension (LVEDD) and decreases in fractional shortening (FS%) at 20 weeks of age. Two-way ANOVA was used to assess effects of timepoint and genotype (full details in Online Table II); * denotes significant difference vs age-matched nontransgenic. For both (A) and (B), data shown are mean \pm s.e.m.; numbers of hearts are shown in columns. (C) Representative M-mode echocardiograms from 20 week-old mouse hearts. (D) Myocyte cross-sectional area shown by fluorescent wheat germ agglutinin staining of 20 week-old mouse hearts. White scale bar represents 10 μ m. Quantitation represents mean values from ~600 myocytes, from each of two hearts. * denotes $P = 0.0004$ relative to nontransgenic (1-way ANOVA).

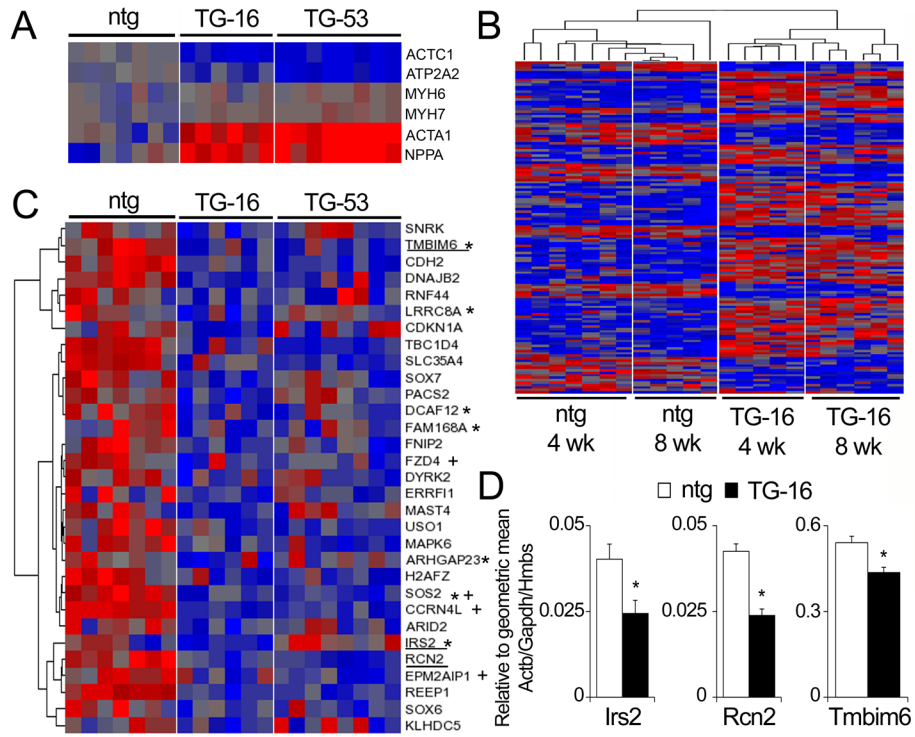


Figure 3. Transcriptome regulation in miR-499 transgenic mice

(A) Markers of the hypertrophic / fetal recapitulation gene program; α -cardiac actin (*Actc1*), SERCA2a (*Atp2a2*), α -MHC (*Myh6*), β -MHC (*Myh7*), α -skeletal actin (*Acta1*) and ANP (*Nppa*) in 4 week-old hearts. (B) Heatmap of 136 mRNAs indirectly regulated by miR-499 in 4 week-old and 8 week-old transgenic hearts (details in Online Table III). (C) Downregulation of 31 miR-499 target mRNAs predicted by TargetScan in miR-499 transgenic hearts (greater than 1.2-fold downregulation, $P < 0.05$, Online Table IV). * denotes downregulation of the same mRNA in human heart failure; + denotes downregulation of the same mRNA in Gaq mice (Figure 1). Underlined mRNAs are those confirmed by RT-qPCR in panel D. Red = higher expression, blue = lower expression. (D) TaqMan RT-qPCR validation of 3 predicted miR-499 target mRNAs. Expression level is normalized to a combined reference⁵⁷ of *Actb*, *Gapdh* and *Hmbs*. Relative abundances of *Irs2*, *Rcn2* and *Tmbim6* correlate to RNA-sequencing determinations (Online Table IV). * denotes $P < 0.05$, unpaired 2-tailed t-test.

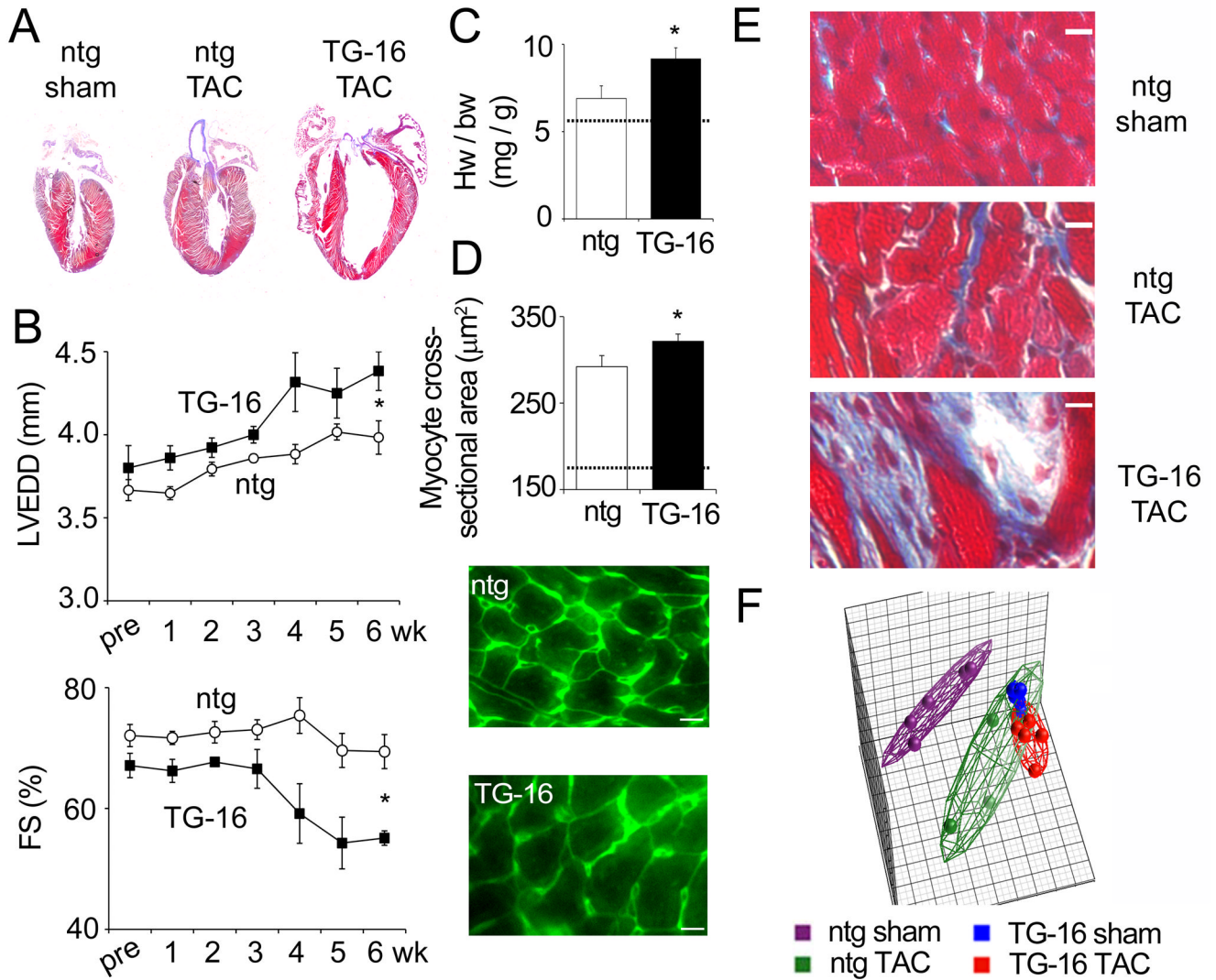


Figure 4. miR-499 overexpression worsens the response to pressure overload in mice (A) Representative sections of nontransgenic sham, nontransgenic pressure-overloaded (TAC) and miR-499 TG-16 pressure-overloaded hearts 6 weeks after surgery. (B) Development of hypertrophy shown by echocardiography of nontransgenic (n=5) and miR-499 TG-16 (n=3) animals. Data shown are mean \pm s.e.m. ; * denotes significant difference at 6 weeks (P=0.03 for LVEDD and P=0.007 for FS%, 2-tailed unpaired t-test). (C) Heart weight / body weight ratios after 6 weeks TAC. * denotes significant difference (P=0.036, 1-tailed unpaired t-test). (D) Myocyte cross-sectional area shown by fluorescent wheat germ agglutinin staining. White scale bar represents 10 μ m. Quantitation represents mean values from ~600 myocytes, from each of 2 hearts. * denotes P=0.04. Dotted lines, C and D: typical levels in age-matched, untreated nontransgenic mice. (E) Fibrosis after 6 weeks of TAC shown by Masson's trichrome staining. White scale bar represents 10 μ m. (F, left) Principal components analysis of 6,500 mRNAs (those expressed at \geq 3 copies/cell) in nontransgenic and miR-499 TG-16 hearts, sham-treated and after 1 week of TAC (5 hearts per treatment). Individual hearts are shown as filled spheres; wireframes enclose all hearts of a treatment group. Reduction of variance to 3 principal components (the 3 dimensions shown in the plot) accounts for 49.8% of the total variance in the data set.

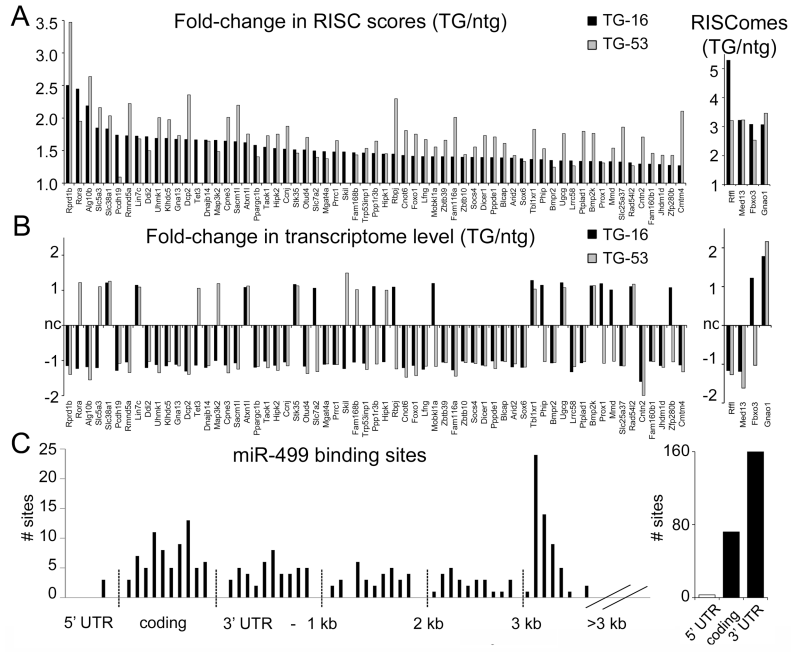


Figure 5. Direct targets of miR-499 in mouse hearts
(A, left) Fold-change in RISC score (RISCome expression/transcriptome expression) between transgenic and nontransgenic mice for 63 direct targets of miR-499 identified by RISC-sequencing. **(A, right)** Change in RISCome expression for a further 4 miR-499 targets. **(B)** Fold-change in transcriptome expression for the miR-499 targets shown in **(A)**. nc = no change. Black bars, miR-499 transgenic TG-16; gray bars, miR-499 transgenic TG-53. **(C)** Schematic depiction of miR-499 recognition sites in miR-499 targets defined by RISC-sequencing. Graph on the left shows number of sites according to mRNA position; graph on the right shows aggregate counts. The majority (68%) of putative binding sites are in the 3' untranslated region (UTR), with 31% in coding regions and 1% in the 5' UTR.

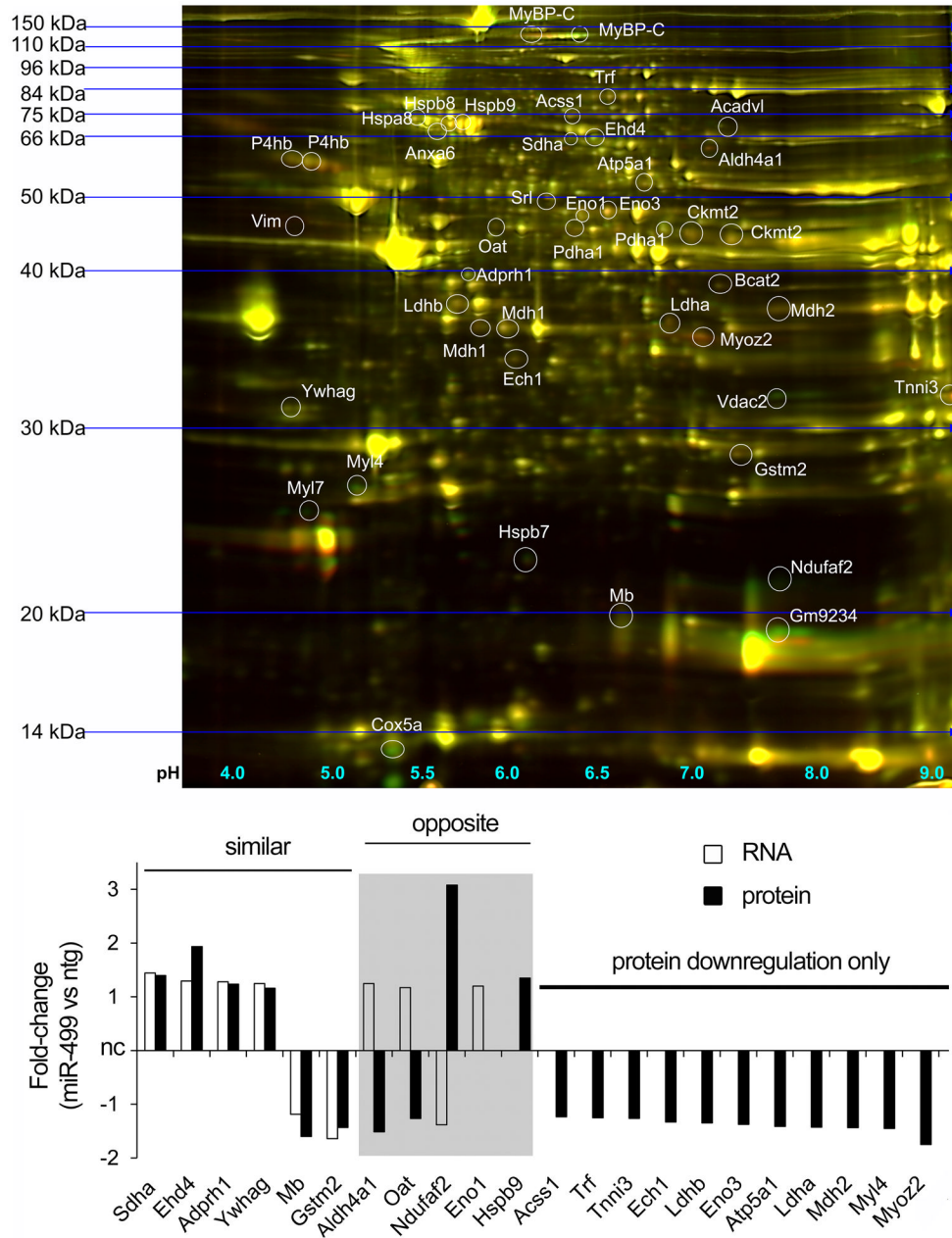


Figure 6. Similar and differential regulation of mRNA and protein for indirect targets of miR-499

Upper panel: Representative 2D DiGE gel image. Green = miR-499, red = nontransgenic cardiac protein. **Lower panel:** Comparison of mRNA and protein regulation for 22 gene products. *Mybpc3* (MyBP-C), *Ckmt2*, *Mdh1*, *P4hb* and *Pdha1* migrated as multiple species and were not analyzed. Also identified, but with neither mRNA nor protein regulation: *Acadvl*, *Anxa6*, *Cox5a*, *Hspa8*, *Hspb8*, *Myl7*, *Vdac2*, *Vim*. White bars, mRNA regulation; black bars, protein regulation. nc = no change. Regulated mRNAs had changes of $\geq 20\%$, $P < 0.05$. Proteins were classed as regulated if changes of $\geq 20\%$ in the same direction were identified on at least 3 of 5 gels.

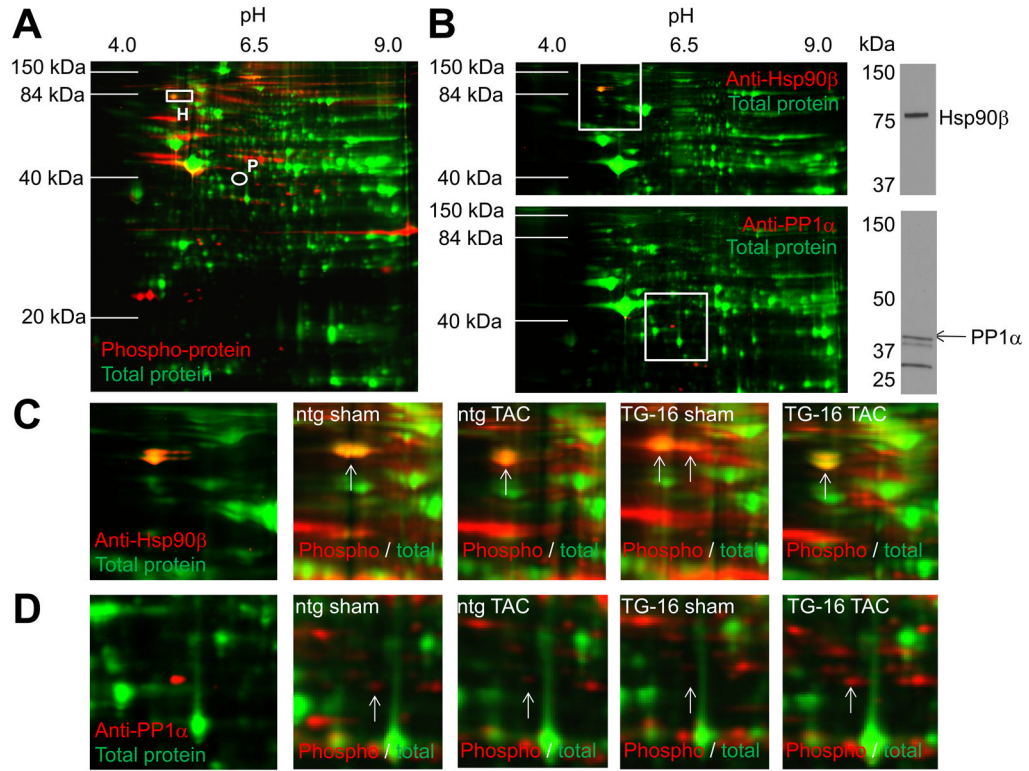


Figure 7. Differential phosphorylation in nontransgenic and miR-499 transgenic mice at 1 week of pressure overload

(A) Representative phosphoproteome 2D gel image of nontransgenic sham-treated cardiac protein samples. Green is total protein stain; red is ProQ-diamond phosphoprotein; rectangle, HSP90β (H); circle, PP1α (P). (B) 2D immunoblots of HSP90β and PP1α; 1D SDS-PAGE of a nontransgenic, sham-treated cardiac protein sample is shown to at right. White squares denote regions shown in panels C and D. (C) Left: magnified view of 2D immunoblot for HSP90β. Right: same region in representative phosphoproteome 2D gels for nontransgenic and TG-16, sham- and TAC-treated hearts. (D) as for (C) but for PP1α. A total of 5 hearts were used in each treatment group (Online Figure VI).

